

Study of the facade degradation agents associated with temperature and driving rain in different Brazilian bioclimatic zones

A. L. Ramos^{1*} , E. Bauer² 

*Contact author: analin.ramos@gmail.com

DOI: <https://doi.org/10.21041/ra.v12i2.560>

Reception: 10/01/2022 | Acceptance: 01/04/2022 | Publication: 01/05/2022

ABSTRACT

Therefore, the aim is to study the conditions of exposure to these degradation agents in buildings located in different Brazilian bioclimatic zones. Knowing the action of weathering is essential to understand the facades degradation. For this purpose, eight cities were selected: Curitiba, Santa Maria, Florianópolis, Brasília, Niterói, Goiânia, Picos and Belém. A model building was defined for hygrothermal simulation to assess total radiation, temperature range, thermal shock, intensity index temperature and driving rain. As a result, zones of critical conditions are identified, providing exposure rankings. For temperature agents and directed rain, the most exposed cities are Goiânia-GO and Belém-PA, respectively. Finally, the mildest exposure zones are Belém-PA for temperature agent and Niterói-RJ for driving rain.

Keywords: degradation; facades; ceramic coating; bioclimatic zones; temperature.

Cite as: Ramos, A. L., Bauer, E. (2022), "*Study of the facade degradation agents associated with temperature and driving rain in different Brazilian bioclimatic zones*", Revista ALCONPAT, 12 (2), pp. 248 – 262, DOI: <https://doi.org/10.21041/ra.v12i2.560>

¹ Aluna de mestrado PECC, Universidade de Brasília, Brasília, Brasil.

² Professor Doutor do PECC, Universidade de Brasília, Brasília, Brasil.

Contribution of each author

In this work, Ana Lin Ramos contributed to the activity of structuring and writing the text (100%), analysis and discussion of the results (100%). Elton Bauer contributed to the activity data collection (100%), supervision (100%) and correction of the text (100%).

Creative Commons License

Copyright 2022 by the authors. This work is an Open-Access article published under the terms and conditions of an International Creative Commons Attribution 4.0 International License ([CC BY 4.0](https://creativecommons.org/licenses/by/4.0/)).

Discussions and subsequent corrections to the publication

Any dispute, including the replies of the authors, will be published in the first issue of 2023 provided that the information is received before the closing of the third issue of 2022.

Estudio de la acción de los agentes de degradación de fachadas asociados a la temperatura y la lluvia dirigida en diferentes zonas bioclimáticas brasileñas

RESUMEN

El objetivo es estudiar las condiciones de exposición a estos agentes degradantes en edificios ubicados en diferentes zonas bioclimáticas brasileñas. Conocer la acción de la meteorización es fundamental para comprender la degradación de las fachadas. Para ello, se seleccionaron ocho ciudades: Curitiba, Santa María, Florianópolis, Brasília, Niterói, Goiânia, Picos y Belém. Se definió un modelo de construcción de simulación higrotérmica para evaluar radiación total, amplitud térmica, choque térmico, índice de intensidad de temperatura y lluvia dirigida. Como resultado, se identifican zonas de condiciones críticas, proporcionando clasificaciones de exposición. Para agentes de temperatura y lluvia dirigida, las zonas más expuestas son Goiânia y Belém. Las zonas de exposición más suaves son Belém para agente de temperatura y Niterói para lluvia dirigida.

Palabras clave: degradación; fachadas; revestimiento cerámico; zonas bioclimáticas; temperatura.

Estudo da ação de agentes de degradação de fachadas associados à temperatura e a chuva dirigida em diferentes zonas bioclimáticas brasileiras

RESUMO

Logo, objetiva-se investigar as condições de exposição a agentes de degradação em edifícios localizados em diferentes zonas bioclimáticas brasileiras. Estudar a ação do intemperismo é essencial para compreender a degradação das fachadas. Selecionou-se oito cidades representativas de cada Zona: Curitiba, Santa Maria, Florianópolis, Brasília, Niterói, Goiânia, Picos e Belém. Definiu-se um edifício modelo para simulação higrotérmica para avaliação da radiação total, amplitude térmica, choque térmico, índice de intensidade da temperatura e chuva dirigida. Como resultado, são identificadas as zonas de condições críticas, que são classificadas em função de sua gravidade. Para temperatura e chuva dirigida, as cidades mais expostas são Goiânia-GO e Belém-PA, respectivamente. As de exposição mais amenas são Belém-PA para agente de temperatura e Niterói-RJ para chuva dirigida.

Palavras-chave: degradação; fachadas; revestimento cerâmico; zonas bioclimáticas; temperatura.

Legal Information

Revista ALCONPAT is a quarterly publication by the Asociación Latinoamericana de Control de Calidad, Patología y Recuperación de la Construcción, Internacional, A.C., Km. 6 antigua carretera a Progreso, Mérida, Yucatán, 97310, Tel.5219997385893, alconpat.int@gmail.com, Website: www.alconpat.org

Reservation of rights for exclusive use No.04-2013-011717330300-203, and ISSN 2007-6835, both granted by the Instituto Nacional de Derecho de Autor. Responsible editor: Pedro Castro Borges, Ph.D. Responsible for the last update of this issue, Informatics Unit ALCONPAT, Elizabeth Sabido Maldonado.

The views of the authors do not necessarily reflect the position of the editor.

The total or partial reproduction of the contents and images of the publication is carried out in accordance with the COPE code and the CC BY 4.0 license of the Revista ALCONPAT.

1. INTRODUCTION

The facade is a constructive element aimed at protecting the building from the external environment and becoming, thus, greatly exposed to factors such as solar radiation, driving rain, and temperature. Such exposure allows a complex degradation process involving agents of different nature that can act in synergy, affecting the performance and useful life of the building components and materials through different degradation mechanisms (Bauer et al., 2021).

The ceramic claddings commonly used on facades are associated with a specific degradation process characterized mainly by tile detachment (Bauer et al., 2015; Pacheco and Vieira, 2017) in addition to cracking, lack of ceramic-substrate adhesion, and expansion of substrates due to humidity or thermal variations (Bezerra et al., 2018). In this case, the layers making up the cladding system have different properties (thermal expansion coefficients, modulus of elasticity, thermal conductivity, etc.) and, thus, the action of agents associated with temperature becomes highly relevant (Gaspar and Brito, 2011).

Additionally, the varying surface temperature of the cladding can cause physical changes in the facade sealing system (Silva, 2000). This degradation mechanism results from the effect of expansion and contraction due to temperature variations and non-homogeneous increments that cause shear stresses, generating a separation tendency at the system interface (Saraiva, 1998). As a result, the detachments and cracks that appear in the ceramic claddings can be intensified by the fatigue caused by thermomechanical efforts derived from temperature variations, in addition to restrictions on deformation (Barbosa, 2013).

The weighted thermal amplitude, represented by the Temperature Intensity Index, as well as solar radiation and thermal shocks are used as a representative value of the thermal amplitude and indicative of a greater degradation. The I_{TI} constitutes an analysis of the thermal amplitude that yields a weighted measurement concerning frequency (Nascimento, 2016) and thermal shock, which are punctual events characterized by a high difference in surface temperature in a short time interval (Zanoni, 2015).

The driving rain acting under the facades is considered a highly relevant agent (Nascimento et al., 2016). This action results from the association between rain and wind and is one of the main sources of water on building facades. Without the action of the wind, the rain would fall vertically without wetting significantly the walls (Zanoni, 2015). However, due to the action of the wind, the rain hits mainly the top and sides of buildings. And, although ceramic claddings suffer less significantly from the precipitation incidence compared to the mortar system (Bauer et al., 2018), it should be considered in hygrothermal simulations to understand the degradation process.

The degradation of ceramic cladding systems is mainly characterized by ceramic detachment, even though the degradation process changes for different geographical locations (Souza, 2019). Therefore, it is necessary to study the conditions of exposure to the actions of climatic agents to understand the different conditions triggering the degradation process in different regions.

As a continental country, Brazil has climatic variations throughout its territory. For this reason, ABNT NBR 15220-3 (2005) establishes the Brazilian bioclimatic zoning by classifying 330 cities according to their climate into eight bioclimatic zones. These zones are defined as homogeneous geographic regions regarding climate elements that interfere with the built environment and human comfort relationship. Buildings and their elements located in different zones are subject to different exposure conditions to the climate agents that cause the degradation process.

The objective of the proposed investigation is to analyze the action of degradation agents associated with temperature and driving rain on the facades of buildings located in different Brazilian bioclimatic zones. Therefore, the hygrothermal simulation performed using the WUFI Pro 6.5 software, a useful tool for studying degradation (Bauer et al., 2018; Gonçalves et al., 2018), allowed to obtain data on incident solar radiation, surface temperature and driving rain on the North facades

of a model building subjected to the different climatic conditions of each zone.

2. METHODS

2.1 Details of the model building.

In this study, the model building is 20m high with a 63.5% absorbance ceramic cladding system (Dornelles, 2007) corresponding to the dark red color, chosen to highlight the effects of temperature, since dark colors present higher surface temperature when exposed to radiation (Uchôa et al., 2016). This model building is placed in different cities located in the eight Brazilian bioclimatic zones as established in the ABNT NBR 15220-3 (2005). Table 1 shows the chosen cities and the corresponding bioclimatic zone.

Table1. City, State and the different bioclimatic zones.

Z1	Z2	Z3	Z4	Z5	Z6	Z7	Z8
Curitiba-PR	Santa Maria-RS	Florianópolis-SC	Brasília-DF	Niterói-RJ	Goiânia-GO	Picos-PI	Belém-PA

2.2 Simulation

The hygrothermal simulation in the WUFI Pro 6.5 software is used to evaluate the action of climatic agents on the facades in each city. The software allows entering data such as simulation period, configuration, orientation and inclination of the construction system, coefficients of driving rain and transfer to the surface, initial conditions of temperature and relative humidity, as well as interior and exterior climatic conditions (Freitas, 2011). The simulation output yields the hourly values of total radiation incident on the facades, surface temperature and precipitation.

The simulation was performed for one year period, between 01/01/2019 and 01/01/2020. The outdoor weather conditions of each city are defined based on the Typical Meteorological Year (TMY) files from the EPW/ANTAC database (Roriz, 2012). Table 2 contains the values adopted for the surface transfer coefficients.

Table 2. Transfer coefficients to the external surface adopted in the simulation.

Coefficient	Unit	Value
Thermal Resistance (left side)	m ² K/W	0.058
Absorption (Shortwave Radiation)	-	0.635
Soil Reflectivity	-	0.2
Incident rain reduction factor	-	0.7

In the study, because all cities studied are below the equator, we chose to analyze only the North facade of each building, which is critical for the incidence of solar radiation. The simulated construction system consists of ceramic cladding, cementitious plastering mortar, ceramic block, internal mortar, and the main monitoring point on the cladding surface. Figure 1 shows the system launched in the program.

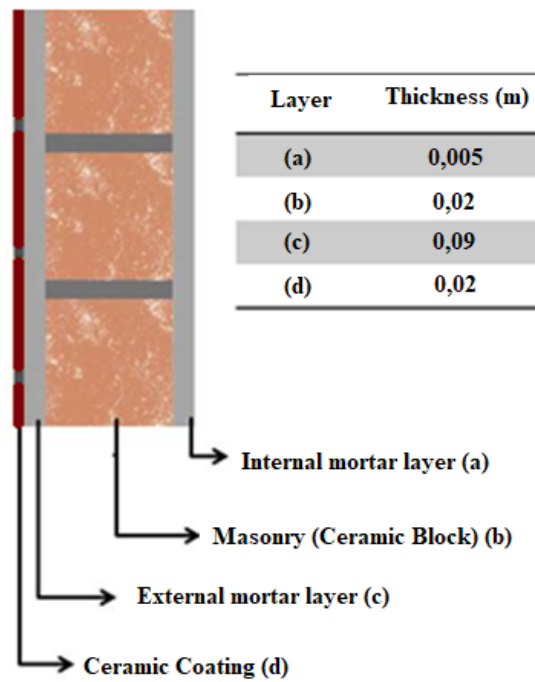


Figure 1. Evaluated constructive system: (a) ceramic tile; (b) external mortar/plaster; (c) ceramic block; (d) internal mortar.

The properties of the materials used in the constructive system layers had already been determined in previous tests conducted by other researchers. The lab tests determined apparent specific mass; porosity; water vapor permeability to calculate the water vapor diffusion resistance factor; water absorption coefficient or capillarity coefficient; and hygroscopic curve. The test results are described in detail in the LEM-UnB Internal Report (Bauer et al., 2015). Table 3 summarizes these results.

Table 3. Summary of material properties.

Properties	Ceramic Block	Ceramic Tile	Plaster Mortar
Apparent specific mass (kg/m ³)	578	1730	1830
Porosity (m ³ /m ³)	0.486	0.29	0.2604
Permeability to water vapor (kg/(m.s.Pa))	8.38. 10 ⁻¹²	1.66. 10 ⁻¹²	7.9. 10 ⁻¹²
Water absorption coefficient (kg/m ² .√s)	0.09	0.001	0.089

2.3 Degradation agents associated with temperature.

2.3.1 Total radiation, maximum and minimum surface temperature and maximum thermal amplitude.

Equation 1 uses surface temperature data to determine the maximum and minimum temperatures, as well as the daily thermal amplitudes over the simulation period. Furthermore, the daily solar radiation data observed on each facade are added to determine the solar radiation accumulated on the facade over the simulation period.

$$\Delta T = t_{m\acute{a}x} - t_{m\acute{i}n} \quad (1)$$

Where ΔT is the thermal amplitude, $t_{m\acute{a}x}$ is the daily maximum surface temperature of the facade, and $t_{m\acute{i}n}$ is the daily minimum surface temperature of the facade.

2.3.2 Thermal shock

Thermal shock is also analyzed in the study of the effects associated with temperature (Zanoni, 2015). For this purpose, the occurrence frequency of the events called full and attenuated thermal shock is determined for all facades during the simulation year. Full thermal shock is defined by a surface temperature difference greater than 8 °C in a 1-hour interval, whereas attenuated thermal shock consists of the same temperature difference verified in a 2-hour interval. The equations for full (2) and attenuated (3) thermal shock are:

$$\Delta T_{ch} = t_n - t_{n-1} \quad (2)$$

$$\Delta T_{ch} = t_n - t_{n-2} \quad (3)$$

The results are shown in graphs of annual occurrence frequency (%) calculated from the relationship between the total number of occurrences of thermal shocks and the number of hours in a year.

2.3.3 Weighted Thermal Amplitude

To analyze the effects associated with temperature, the weighted thermal amplitude expressed as I_{IT} is calculated for all facades, considering the effects of cycles and surface temperature values reached in the systems (Nascimento, 2016). The I_{IT} is established based on temperature variations and their frequency of occurrence in a given pre-established interval. To do so, the variation range of thermal amplitude is divided into four equal intervals, represented by average amplitude values. The I_{IT} is calculated as a weighted average from the frequency values verified for the climate of Brasilia in the given time interval of one year in this study.

Table 4 shows the ranges of the thermal amplitude variation distributed in four equal intervals (Nascimento, 2016) as follows: below 11.5°C (range 1) to greater than 27.7°C (range 4). Finally, I_{IT} is calculated as shown in (4).

Table 4. Thermal amplitude ranges considered for calculating I_{IT} .

Range	$\Delta T(^{\circ}C)$	ΔT mean ($^{\circ}C$)
4	>27.7	31.8
3	19.7 a 27.7	23.7
2	11.5 a 19.6	15.6
1	< 11.5	7.5

$$I_{IT} = \sum \frac{\Delta T_{mean} \times f_n}{f_{total}} \tag{4}$$

Where I_{IT} is the temperature intensity index (°C), ΔT_{mean} is the amplitude of the average temperature in the range of occurrence (°C), f_n is the occurrence frequency of range “n” of ΔT , and f_{total} is the frequency of all occurrences of the four study ranges in the year, i.e., $f_{total} = 365$.

2.3.4 Driving rain

The driving rain is studied using the WUFI software, in which hourly values of precipitation, wind speed and direction are obtained for a total of 8760 hours and used as input data in the computer simulations (Zanoni, 2015). From this, the intensity of driving rainfall is calculated using equation (5).

$$R_{wdr} = R_2 \cdot R_h \cdot V \cdot \cos(D - \theta) \tag{5}$$

Where R_{wdr} is the intensity of driving rain (mm/h); R_h is precipitation on a horizontal surface (mm); R_2 is the coefficient dependent on the location on the facade (s/m); V is the hourly average of wind speed at a height of 10m (m/s); D is wind direction (angle from the North); θ facade orientation measured as the angle between the north and the direction normal to the wall.

In the WUFI quantification methodology, the value of R_2 depends on the building height and the location of the study area of the facade as shown in Table 5. In this study, we adopted the value of 0.2 for tall buildings, upper part taller than 20 m. The simulation output data are the values of precipitation incidents on the facades while the annual accumulated driving rain expressed as l/m² is calculated.

Table 5. R_2 values tabulated in the WUFI quantification methodology.

Height	R_2
Small building, height up to 10 m	0.07
Tall building, lower part up to 10 m	0.05
Tall building, middle part between 10 and 20 m	0.1
Tall building, upper part greater than 20 m	0.2

3. RESULTS

3.1 Total radiation, maximum surface temperature and maximum thermal amplitude.

The results of the total incident radiation and the absolute maximum surface thermal amplitudes on the North facades of the eight zones are shown in Figure 2. It is noted that the highest values occur in Z6 (38.15°C) followed by Z2 (37.5°C) and Z1 (37.15°C), whereas the lowest value is found in Z8 (22.64°C) and intermediate values were observed in the other zones. The highest solar radiation incidence is observed in Z4 (1,014,409 W/m²) followed by Z6 (995,347 W/m²) while Z8 has the lowest value (743,527 W/m²). Additionally, the solar radiation incidence is associated with the temperature gain on each facade, especially in the Z8 and Z6 zones, except for Z4, which had the highest radiation incidence and the third lowest thermal amplitude.

Total radiation is critical in Z4 and Z6, whereas exposure conditions are milder in Z8, despite being

close to the equator and represented by Belém, in PA. This result is because the solar radiation incident on the facade is only a portion of the horizontal global solar radiation (consisting of the direct, diffuse and reflected components) (Silva, 2011) dependent, therefore, on facade orientation and slope.

The surface temperature and the thermal amplitude at the surface result from the interaction between solar radiation and the rise in air temperature throughout the day, thus being better indicators of hygrothermal variations than the total incident solar irradiation (Zanoni, 2015). In this case, Z6 and Z7 are critical zones, as they have a higher thermal amplitude (Figure 2) and higher surface temperature (Figure 3) throughout the year, respectively.

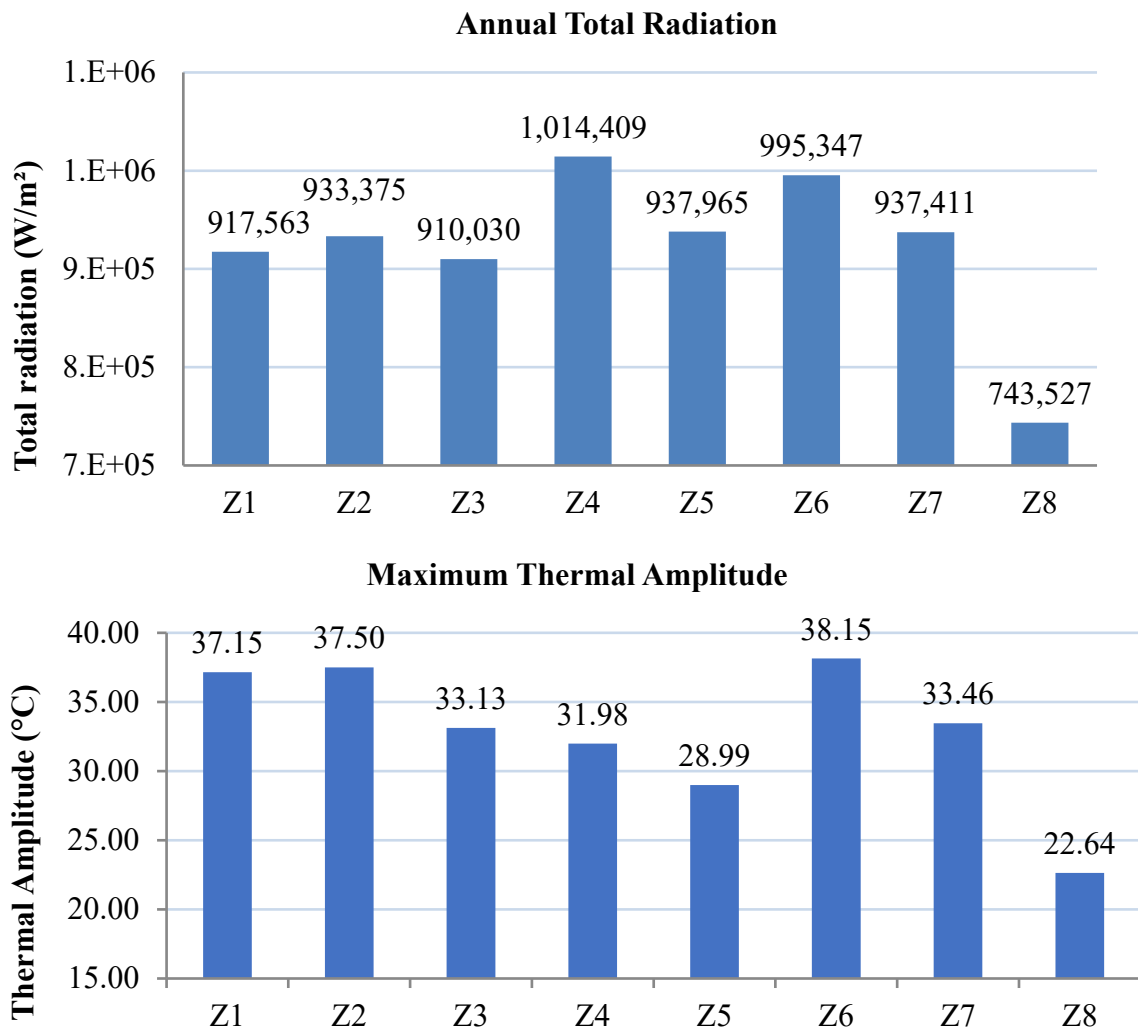


Figure 2. Total accumulated radiation and maximum thermal amplitude in the simulation year.

The annual maximum and minimum temperatures for each of the studied facades are shown in Figure 3. It is noted that the lowest temperatures, measured when there is no incident radiation on the facade, vary greatly in the studied buildings. The lowest temperatures of 2.99°C, 5.48°C and 6.98°C were measured for Z2, Z1 and Z3, respectively. Meanwhile, Z8, despite having a lower incidence of total radiation on the facade, has a higher minimum (22.07°C) and a lower maximum (46.16°C) temperature, which is consistent with reduced thermal amplitudes, as shown in Figure 2. In this case, it is emphasized that the surface temperature is linked not only to the incidence of radiation on the facade but also to the air temperature (ASHRAE, 2009; Lamberts et al., 2011).

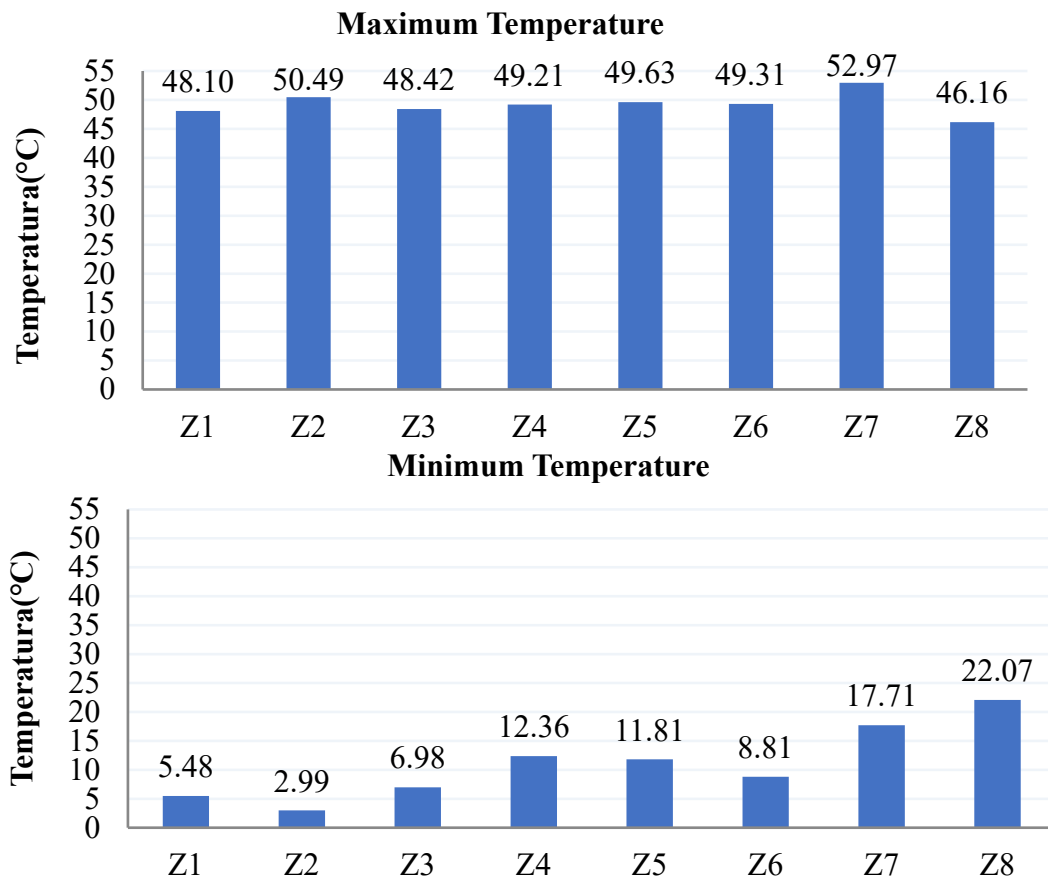


Figure 3. Absolute maximum and minimum surface temperatures for each bioclimatic zone in the studied year.

3.2 Thermal shock.

Figure 4 shows the occurrence frequency of full thermal shocks on all facades. The highest frequency is observed in Z6, in which 1.59% of the measurements are characterized as full thermal shocks, followed by Z1 (0.92%) and Z4 (0.79%). Zones Z5 and Z7 had the lowest frequencies 0.16% and 0.19%, respectively.

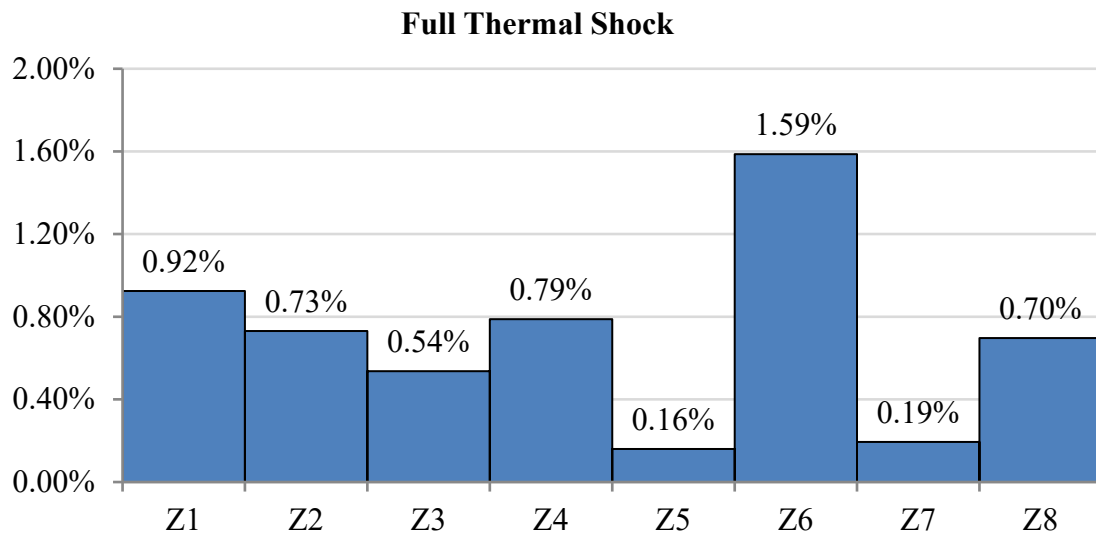


Figure 4. Frequency of occurrence of full thermal shock during one year.

The full thermal shock peaks are more frequent between May and July, according to Table 6. The monthly distribution of the number of shocks over a year indicates the month with the highest frequency of thermal shocks for each zone. Thus, the data show that the occurrence frequency of full thermal shocks peaked in zones Z1 and Z5 in July; Z3, Z4, Z6 and Z7 in June; and Z2 and Z8 in May. In zones 1 to 7, thermal shocks decreased from October to March, reaching zero in one or more months during this period except for Z8, where thermal shock events are better distributed throughout the year.

Table 6. Number of monthly full thermal shock events during one simulation year.

Full thermal shock													
	Jan	Feb	Mar	Apr	May	Jun	Jul	Aug	Sept	Oct	Nov	Dec	sum
Z1	1	1	1	9	14	18	25	9	1	1	0	1	81
Z2	0	1	0	4	21	10	7	12	7	0	0	2	64
Z3	1	0	0	1	6	25	14	0	0	0	0	0	47
Z4	1	1	0	4	17	23	19	0	0	1	0	3	69
Z5	0	0	0	0	1	5	6	1	1	0	0	0	14
Z6	4	1	3	10	13	53	38	12	0	0	1	4	139
Z7	0	1	3	3	2	6	2	0	0	0	0	0	17
Z8	5	5	6	7	10	5	2	3	1	4	5	8	61

The frequency of attenuated shocks is shown in Figure 5. the highest frequency of 13.65% is observed in Z6, followed by Z4 with 10.88%. Z8, Z5 and Z2 have the lowest frequency values of 2.84%, 3.35% and 4.95%, respectively. It is noteworthy that Z6 has approximately 5 times more attenuated shocks than Z8. The frequency is also high in Z4 and Z1 (10.88% and 10.31%, respectively) followed by Z3 and Z7 (8.75% and 8.60%).

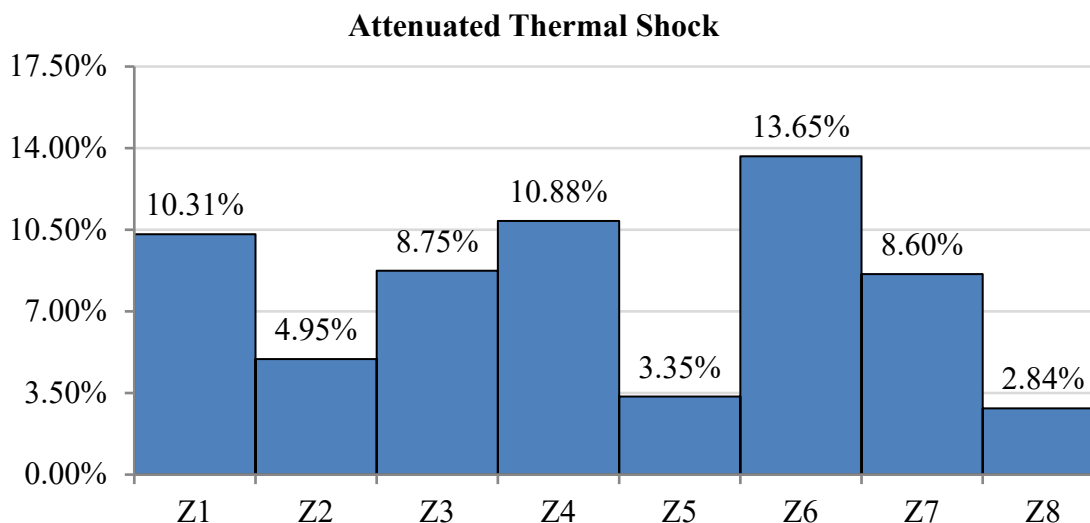


Figure 5. Frequency of attenuated thermal shock observed in one simulation year.

The annual distribution shows higher occurrence from May to August, as observed in Table 6. Only Z5 has two months without the occurrence of thermal shocks (November and December). The occurrence peaked in Z2 and Z8 in May; Z4 and Z6 in June; Z1, Z5 and Z7 in July; and Z3 in August. The occurrences in Z8 are better distributed throughout the year, varying from 12 in September to 32 in May. Meanwhile, in other areas, variation between the months of lowest and highest occurrence is greater, such as in Z6, where it varied from 14 events in November to 211 events in June.

Table 7. Monthly frequency of attenuated thermal shock events over a simulation year.

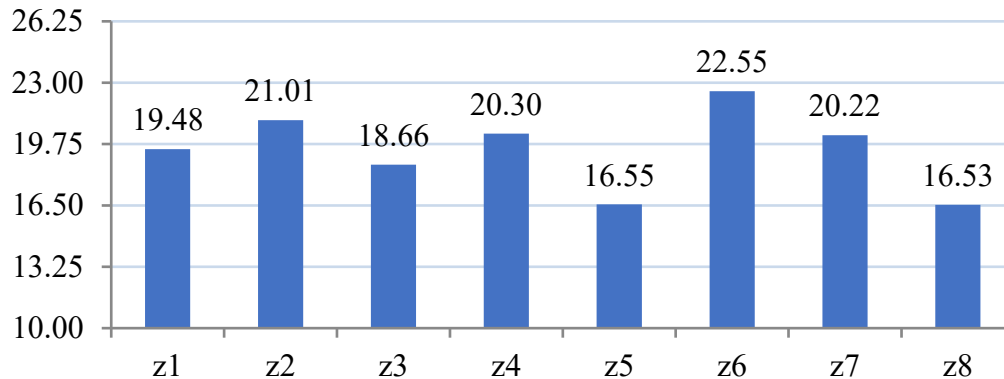
Attenuated Thermal Shock													
	Jan	Feb	Mar	Apr	May	Jun	Jul	Aug	Sept	Oct	Nov	Dec	sum
Z1	13	24	64	112	146	103	190	114	78	46	4	9	903
Z2	6	14	39	65	85	38	50	62	44	27	1	3	434
Z3	6	25	72	106	127	115	76	128	73	28	5	5	766
Z4	6	18	52	120	148	182	177	143	71	16	10	10	953
Z5	2	1	5	32	46	56	82	44	22	3	0	0	293
Z6	27	33	76	121	175	211	207	170	84	56	14	22	1196
Z7	10	11	32	80	155	145	157	114	40	3	2	4	753
Z8	18	15	22	29	32	20	29	19	12	18	14	21	249

The results show that zones with critical exposure have the highest frequency of thermal shock and those exposed to milder conditions have the lowest frequency. Zone Z6 stands out since it presented the highest frequency for both full and attenuated thermal shocks. Finally, Z5 had a reduced frequency of both thermal shocks considered while Z8 had a lower frequency of attenuated shocks.

3.3 Weighted Thermal Amplitude.

Figure 6 shows the I_{IT} results for all facades in each bioclimatic zone. The results take into account the temperature gradient during one year of simulation. As noted in the results of maximum thermal amplitude and thermal shock, Z6 presents critical values (22.55) regarding the action of temperature agents. Also, Z8 and Z5 have the lowest I_{IT} values (16.53 and 16.55) whereas Z2, Z4 and Z7 present high values, and zones Z3 and Z1 present intermediate values.

IIT

Figure 6. I_{IT} values for all bioclimatic zones.

Thermal variations on the facades cause deformations in the cladding system and induce fatigue stresses as a result of its cyclic nature. Thus, thermal variations are related to anomalies in facade cladding, especially concerning ceramic detachment and cracking (Silva, 2014; Souza, 2016). I_{IT} is considered a reference value for comparing degradation levels between cities that demonstrates the severity of exposure to the thermal degradation agent. Therefore, higher values indicate greater exposure and greater potential for degradation and decreasing useful life.

The I_{IT} is considered adequate to correlate the degradation of facades (Nascimento, 2016), and, based on these index values, we ranked the facades regarding exposure to temperature, according to severity. Then, in descending order, the areas of greatest severity were: Z6-Z2-Z4-Z7-Z1-Z3-Z5-Z8.

3.4 Driving rain.

Figure 7 shows the incidence of total annual rainfall (l/m^2) on the same North-facing facades to complete the analysis of the degradation agents. Note that Z8 has a critical total annual rainfall ($113.15 l/m^2$), the value is about 6 times higher than the lower incidence observed in Z5 ($18.2 l/m^2$), in contrast to the previous results. Rainfall is also high in Z4 ($100.12 l/m^2$) and Z3 ($71.72 l/m^2$) compared to the others. Finally, Z1 ($52.19 l/m^2$) and Z6 ($59.67 l/m^2$) present intermediate values while Z2 ($35.57 l/m^2$) and Z7 ($30.57 l/m^2$) have a lower incidence of rain.

Total Annual driving Rain

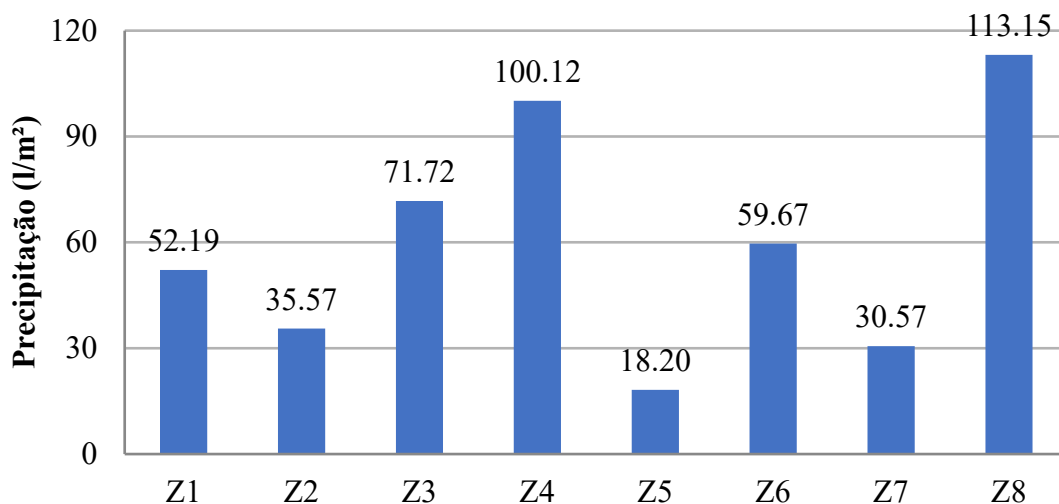


Figure 7. Accumulated driving rainfall in all bioclimatic zones during one year.

It is noteworthy that driving rain results from the action of winds on the precipitation (Freitas, 2011; Zanoni, 2015), therefore, it depends on wind speed and direction. The Northern rainfall incidence is highest in Brasilia and Goiania (Zanoni et al., 2014; Zanoni et al., 2018; Andrade et al., 2021; Melo and Carasek, 2011). The Eastern rainfall incidence is highest in Curitiba (Batista et al., 2017) while the Southern rainfall is most common in Florianópolis (Giango et al., 2010; Giongo, 2007). In this case, the results presented do not necessarily represent the orientation of critical exposure to moisture from the rain, but the orientation adopted as a reference, North.

4. CONCLUSION

This study investigated the action of degradation agents associated with temperature driving rain on the facades of buildings located in Brazilian cities from different bioclimatic zones. In this context, it was possible to identify areas that are critical regarding the exposure to degradation agents as a way of contributing to the knowledge of the different conditions that trigger the degradation process in Brazil. The results allowed us to identify the following patterns:

- Zone Z6 represented by Goiânia-GO had the most critical response to the exposure conditions regarding thermal amplitude, attenuated and full thermal shock, and temperature intensity index;
- Zone Z8 represented by Belém-PA, despite exhibiting a milder response to exposure conditions to the agents associated with temperature (solar radiation, thermal amplitude, attenuated thermal shock and temperature intensity index) is critical for exposure to the driving rain.
- Zones Z1, Z2, Z3, Z5 and Z7 represented by Curitiba-PR, Santa Maria-RS, Florianópolis-SC, Niterói-RJ and Picos-PI, respectively, presented similar values of total annual radiation incidence on the North facade. However, zones Z1 and Z2 present higher thermal amplitudes compared to the others.
- Regarding driving rain and considering the annual precipitation values, the North facades in Z8 (Belem-PA) and Z4 (Brasília-DF) presented higher exposure while Z5 had the mildest exposure.
- It is concluded that the North facades analyzed in the 8 Brazilian bioclimatic zones have different exposure conditions to agents associated with temperature and driving rain. These parameters affect building durability since the synergy between degradation agents acting on the facades accelerates the degradation, compromising building performance and affecting useful life. In addition, as a contribution, the study ranks the studied regions regarding the severity of exposure to temperature and, therefore, with greater potential for degradation and decreasing useful life. In descending order, the most exposed zones are: Z6-Z2-Z4-Z7-Z1-Z3-Z5-Z8 represented by the cities Goiânia-Santa Maria-Brasília-Picos-Curitiba-Florianópolis-Niterói-Belém.

5. ACKNOWLEDGEMENTS

We are grateful to the PECC (Postgraduate program in structures and civil construction) University of Brasília, and the DMMPROJECT (Degradation: Measurement and Modelling). This study was financed in part by the Coordenação de Aperfeiçoamento de Pessoal de Nível Superior - Brasil (CAPES) – Finance Code 001, by the Conselho Nacional de Desenvolvimento Científico e Tecnológico (CNPq), and by Academic Dean Graduate Studies (DPG) of the University of Brasilia (UnB).

6. REFERENCES

- Andrade, D., Kardec, T., Bauer, E.(2021). “*Sinergia dos agentes higrotérmicos na degradação de fachadas*”. In: XVII Congresso Internacional sobre Patologia e Reabilitação das construções, 2021, Fortaleza.
- ASHRAE - American Society of Heating (2009), *Refrigerating and Air-Conditioning Engineers*, Inc. Handbook 2009 -Fundamentals. Atlanta, artigo 2SPPC1017, pp. 199–212, 2017.
- Associação Brasileira de Normas Técnicas (2005). *NBR 15220-3: Desempenho térmico de edificações Parte 3: Zoneamento bioclimático brasileiro e diretrizes construtivas para habitações unifamiliares de interesse social*. Rio de Janeiro.
- Barbosa, A. S. (2013), “*Estudo Numérico-Computacional e Analítico do Choque Térmico em Fachadas de Edificações*”. Dissertação (Mestrado). Masters Thesis, Programa de Pós-Graduação em Estruturas e Construção Civil, Universidade de Brasília, Brasília-DF.
- Batista, G., Rufato, R., Miranda, D., Giordano, D. Medeiros, M. (2017), “*Análise do índice de chuva dirigida em cidades do Paraná e sua importância no projeto de fachadas de edifícios*”. IN: Simpósio Paranaense de Patologia das construções, 2017.
- Bauer, E., Aidar, L. A. G., Piña, A. B. S. (2018), “*Estudo do transporte de água oriunda da chuva dirigida em fachadas – aplicação com o emprego da simulação higrotérmica*”. IN: Construção, 2018, Brasília, Livro de Atas.
- Bauer, E., Castro, E. K., Silva, M. N. B. (2015), “*Estimativa da degradação de fachadas com revestimento cerâmico: estudo de caso de edifícios de Brasília*”. *Cerâmica*, v. 62, p. 151-159. <https://doi.org/10.1590/0366-69132015613581786>
- Bauer, E., Mota, L., Souza, J. (2021). “*Degradação de fachadas revestidas em argamassas nos edifícios de Brasília, Brasil*”. *Ambiente Construído*, Porto Alegre, v. 21, n. 4, p. 23-43. <http://dx.doi.org/10.1590/s1678-86212021000400557>
- Bauer, E., Nascimento, M. L. M., Castro, E. K.(2015), “*Parâmetros e ensaios físicos de materiais e componentes da fachada. Relatório interno*” – Laboratório de Ensaio de Materiais (LEM) – UnB/ENC.
- Bezerra, L. M., Uchôa, J. C., Araújo, J. A., Bonilla, J. (2018), “*Experimental and Numerical Investigation of Fatigue in Base-Rendering Mortar Used in Façades Undergoing Thermal Cycles*”. *Journal of Materials in Civil Engineering*. v. 30. n. 8. pp.1-14. [https://doi.org.ez54.periodicos.capes.gov.br/10.1061/\(ASCE\)MT.1943-5533.0002319](https://doi.org.ez54.periodicos.capes.gov.br/10.1061/(ASCE)MT.1943-5533.0002319)
- Dornelles, K. A., Roriz, M. (2007), “*A ilusão das cores na identificação da absorvância solar de superfícies opacas*”. In: IX ENCAC E VII ELACAC, 2007, Ouro Preto. Anais. Ouro Preto: ANTAC.
- Freitas, A. S. S. L. A. (2011), “*Avaliação do comportamento hidrotérmico de revestimentos exteriores de fachadas devido à acção da chuva incidente*”, Masters Thesis. Faculdade de Engenharia da Universidade do Porto. Porto, Portugal. 170 p.
- Gaspar, P., Brito, J. (2005), “*Mapping Defect Sensitivity in External Mortar Renders*”. *Journal of Construction and Building Materials*, v. 19(8), p. 571-578, 2005. <https://doi.org/10.1016/j.conbuildmat.2005.01.014>
- Giongo, M. (2007), “*Análise do nível de exposição das edificações à chuva dirigida para Florianópolis*”. Masters Thesis, Universidade Federal de Santa Catarina, 2007.
- Giango, M., Padaratz, I. J., Lamberts, R. (2011), “*Determinação da exposição à chuva dirigida em Florianópolis, SC: índices de chuva dirigida e métodos semi-empíricos*”. *Ambiente Construído*, v. 11, n. 1, p. 7-23. <https://doi.org/10.1590/S1678-86212011000100002>
- Lamberts, R (2011). “*Desempenho térmico de edificações. Apostila da disciplina ECV 5161 do LABEEE-Laboratório de Eficiência Energética em Edificações*”. Universidade Federal de Santa Catarina, Florianópolis, 2011.

- Melo, C. M., Carasek, H. (2011), “Índices de chuva dirigida direcional e análise do nível de umedecimento em fachadas de edifício multipavimentos em Goiânia, GO”. *Ambiente Construído*, v. 11, n. 3, p. 23-37. <https://doi.org/10.1590/S1678-86212011000300003>
- Moscoso, Y. F. M. (2013), “Estudo numérico e experimental de tensões atuantes na argamassa colante de fachadas de edificações sob ação da fadiga termo-mecânica”. Masters Thesis, Universidade de Brasília, Brasília. p. 142.
- Nascimento, M. (2016), “Aplicação da simulação higrotérmica na investigação da degradação de fachadas de edifícios”, Masters Thesis, Universidade de Brasília, Brasília, 2016.p. 127
- Nascimento, M. L. M., Bauer, E., de Souza, J. S. (2016), “Wind-driven rain incidence parameters obtained by hygrothermal simulation”. *Journal of Building Pathology and Rehabilitation* 1, 5. <https://doi.org/10.1007/s41024-016-0006-5>.
- Pacheco, C. P., Vieira, G. L. (2017), “Análise quantitativa e qualitativa da degradação das fachadas com revestimento cerâmico”. *Cerâmica*, v. 63, p. 432-445. <https://doi.org/10.1590/0366-69132017633682156>
- Roriz, M. (2012), “Correções nas Irradiâncias e Iluminâncias dos arquivos EPW da Base ANTAC”. Grupo de Trabalho sobre Conforto e Eficiência Energética de Edificações. ANTAC – Associação Nacional de Tecnologia do Ambiente Construído. São Carlos – SP.
- Saraiva, A. G. (1998), “Contribuição ao Estudo de Tensões de Natureza Térmica em Sistemas de Revestimento Cerâmico de Fachada”. Masters Thesis. Universidade de Brasília. Brasília, Brasil. 164 p.
- Silva, A., Dias, J. L., Gaspar, P. L., Brito, J. (2011), “Service life prediction models for exterior stone cladding”. *Building Research and Information*, 39(6): 637-653, 2011. <https://doi.org/10.1080/09613218.2011.617095>
- Silva, M. N. B. (2000), “Avaliação Numérica com o Método dos Elementos Finitos das Tensões Termo-Mecânicas em Sistemas de Revestimento de Fachadas”. Universidade de Brasília. Brasília, Brasil. 218 p.
- Souza, J. (2019), “Impacto dos fatores de degradação sobre a vida útil de fachadas de edifícios”, Doctoral thesis, Universidade de Brasília, Brasília, Brasil, p. 101.
- Uchôa, J. C. B., Bezerra, L. M., Brito, M. A. N., Júnior, A. C. M., Silva, W. T. M. (2016), “análise de tensões internas em sistemas de revestimentos Cerâmicos de fachadas no distrito federal devido a Carregamentos térmicos utilizando modelagem MEF 3D”. IN: XXXVII Iberian Latin-American Congress on Computational Methods in Engineering, Brasília, DF, Brazil, November 6-9.
- Zanoni, V. (2015), “Influência dos agentes climáticos de degradação no comportamento higrotérmico de fachadas em Brasília”. Doctorial Thesis, Universidade de Brasília, Brasília, 2015. p. 253.
- Zanoni, V., Sánchez, J., Bauer, E. (2014), “Chuva dirigida: um estudo da iso 15927-3 no contexto brasileiro. In: XV Encontro Nacional de Tecnologia do Ambiente Construído, 2014, Maceió-AL.
- Zanoni, V., Sánchez, J., Bauer, E. (2018), “Avaliação de métodos para quantificação de chuva dirigida nas fachadas das edificações”. *PARC Pesquisa em Arquitetura e Construção*, Campinas, SP, v. 9, n. 2, p. 122-132, jun. 2018. ISSN 1980-6809. <https://doi.org/10.20396/parc.v9i2.8650260>